16. DEVELOPMENT OF LOW-SHOCK PYROTECHNIC SEPARATION NUTS

By Laurence J. Bement

NASA Langley Research Center
Hampton, Virginia

and

Dr. Vernon H. Neubert

Pennsylvania State University
University Park, Pennsylvania

SUMMARY

"Pyrotechnic shock," a relatively unknown environment generated by the actuation of pyrotechnic devices, has been an increasing concern to aerospace systems designers as system complexity increases. This study has expanded the understanding of pyrotechnic shock in three areas: pyrotechnic separation nuts, a relative idea of their input into structure, and performance monitoring systems. Performance demonstrations and comparisons were made on six flight-type pyrotechnic separation nut designs, two of which are standard designs in current use, and four of which were designed to produce low shock on actuation. Although the shock performances of the four low-shock designs are considerably lower than the standard designs, some penalties may be incurred in increased volume, weight, or complexity. These nuts, and how they are installed, can significantly influence the pyrotechnic shock created in spacecraft structures. A high-response monitoring system has been developed and demonstrated to provide accurate performance comparisons for pyrotechnic separation nuts.

INTRODUCTION

Pyrotechnic shock, the name given to the mechanical pulses created by the actuation of pyrotechnic devices (separation nuts, valves, pin-pullers), has been a poorly understood environment throughout the years of pyrotechnic applications. As spacecraft have become more sophisticated and delicate, the concern caused by this environment has increased. Few anomalies have been directly attributed to these short-duration, high-force, high-frequency pulses; electrical relays chattered on the Apollo program and Titan vehicle, and a commutator failed on a spacecraft prior to a NASA Wallops launch. The unknowns in this pyrotechnic-shock environment have been: How is it generated and transmitted; how is it measured; what are its shapes; what are its effects on spacecraft systems; what can be done to minimize its generation; and can systems be "qualified" under this environment?

The objective of this study was to provide a better understanding of the pyrotechnic-shock environment by demonstrating the performance of four "low-

shock" pyrotechnic separation nut designs, comparing their shock performances to two standard nuts currently in use, relating the mechanical output of all six nut types to their internal mechanisms, and considering their application on aerospace systems. The pyrotechnic-shock performance comparisons and analyses were based on a monitoring system utilizing high-response strain gages, as well as conventional accelerometers, mounted on simple, cylindrical bars.

APPARATUS

The experimental apparatus consists of the monitoring system and seven separation nuts, six flight-type and one nonflight type.

Monitoring System

The main elements of the monitoring system shown in figure 1 are the two cold-rolled steel bars, 3.66 m (12 ft) long and 2.54 cm (1 in.) in diameter. Each was hung by 152.4-cm (60-in.) cables with elastic cords contacting the bars. The shock waves generated by the separation nuts travel in a uniform plane wave down the bar at sonic velocity. Therefore, a time period of 1.44 milliseconds is required for a wave to traverse the 3.66-m (12-ft) length and return to its source, allowing a pulse within that duration to be viewed as a single pulse.

Several adapters were machined to accommodate the stud thread sizes, thread nomenclature 7/16-20 or 1/2-20, and lengths. Also, a cylindrical adapter with a half-inch wall was machined to allow the monitoring of shock waves through the flange of the separation nuts. All separation nuts, except Low-Shock Design 4, utilized this adapter. Low-Shock Design 4 had no mounting flange and the bar was threaded into a tapped portion of the nut's cap. This technique considerably improved the coupling of the nut's generated shock over the flange mounted approach. A 0.32-cm (1/8-in.) flat washer, 8.1 cm (3.2 in.) in diameter, was installed at the nut-to-stud interface to provide a method of containing the internal components of two of the nut designs, Standard Design 1 and Low-Shock Design 1.

The shock waves were monitored by strain gages and accelerometers at positions indicated in figure 1. The strain gages were mounted at diametrically opposing positions on the bars and were wired within the Wheatstone bridge of the amplifier to cancel the effects of longitudinal bending of the bars. The gages, Baldwin Model FAB1235S13, and the amplifiers, Ellis Model BAM-1B, have a frequency response flat to at least 100 kHz. The accelerometers, Endevco Model 2225C, have a resonant frequency of 80 kHz and a mounted resonant frequency of approximately 50 kHz, yielding a monitoring capability that is flat to 10 to 16 kHz. The accelerometer amplifiers were Endevco Model 2718.

The dynamic pulses were recorded on an FM magnetic tape recorder Minneapolis Honeywell 7600 with a frequency response flat to 40 kHz (capable of measuring rise times to 6 μsec). The equivalent paper speed of the permanent records, achieved by reducing playback speeds, was over 5588 cm/sec (2200 in./sec), or 0.19 millisecond/cm (0.48 millisecond/in.).

Separation Nuts

One nonflight and six flight-type separation nuts were tested in this program: a noncaptive design which was historically the first and simplest release nut concept, two "Standard" designs that have been utilized considerably in present and past aerospace programs, and four "Low-Shock" designs that were specifically designed toward reducing the mechanical shock generated on actuation. Although each nut could contain two cartridges for redundancy, only one cartridge was used for each functioning.

The following explanations describe only principles. Physical designs and performance margins are beyond the scope of this presentation.

Noncaptive (see fig. 2).- The bolt is retained by the threaded portion of the steel collet which is in four segments. The segments are, in turn, held in position by a retaining ring. Electrical ignition of the gas-generating cartridge, which produces 6.8948 kN/m^2 (1000 psi) in a 10-cc closed volume, pressurizes the volume formed by the bolt end and the housing. The housing is forced to the right, stripping back the retaining ring and releasing the collet segments. No effort is made for confinement of gases, housing, nor collet segments.

Standard Design 1 (see fig. 3).- This release mechanism is similar to that of the noncaptive nut; the retaining cylinder holds the collet assembly at its base and is withdrawn. The collet in this design has four deep incisions, instead of being segmented. The SBASI (Single Bridgewire Apollo Standard Initiator), which produces 4.4816 kN/m^2 (650 psi) in a 10-cc volume, pressurizes the volume formed by the piston and the retaining cylinder, causing the cylinder to stroke to the right. The piston holds the nut segments in position. As the restraining ring strokes over the collet, the flared portion of the collet is compressed, forcing the base of the collet to petal open, hinging at the base of the incisions, and releasing the bolt. The restraining piston is decelerated by the O-ring as it impacts against the housing.

Standard Design 2 (see fig. 4).- The retaining cylinder holds the segmented collet at two circumferential points of increased diameter. The spreader piston is spring loaded to restrain and spread the segmented collet on its release. The cartridge, which produces 9.6527 kN/m^2 (1400 psi) in a 10-cc volume, pressurizes the volume formed by the housing and the top of the restraining cylinder. This forces the restraining cylinder to the left, allowing the four collet segments to fall into the cylinder's recessed areas, releasing the bolt. The restraining cylinder then impacts against the bottom of the housing.

Low-Shock Design 1 (see fig. 5).- This nut is a modification of Standard Design 1 and utilizes the same release mechanism; the restraining cylinder strokes to the right on pressurization from the output of a SBASI, compressing the incised collet. The shock-reduction principles were to use an increased mass for the pistons, to minimize their acceleration and to maximize the restraining cylinder's acceleration, and to use crushable honeycomb to reduce the peak load forces on the piston and retaining cylinder from the brisant output of the SBASI. This would reduce the pressure-induced loads through the collet into the bolt. The outer honeycomb provides for a longer period of deceleration on impact.

Low-Shock Design 2 (see fig. 6).- The output of the SBASI cartridge is ported into the body of the nut to force the restraining cylinder to the right, releasing the three-segmented collet. The deceleration of the retaining cylinder/spreader piston/collet combination is achieved by the force produced by the residual gases from the output of the cartridge.

Low-Shock Design 3 (see fig. 7).- The output from the SBASI cartridge is ported through the body of the hinging piston to force the retaining cylinder to the right. As the retaining cylinder strokes, the three-segment collet is first released at its base and is then forced to rotate open about the hinging piston by contacting the lower lip of the recessed area in the retaining cylinder. Again, the motion of the retaining cylinder/hinging piston/collet combination is decelerated by the residual gas from the output of the cartridge.

Low-Shock Design 4 (see fig. 8).- The output of the cartridge, which produces 16.272 kN/m^2 (2360 psi) in a 10-cc closed volume, is ported to the annular ports at each end of the nut body. The two retaining cylinders are forced inward, allowing the three-segmented collet to fall into the recessed areas under the force of an expansion spring (not shown). The shock-reduction principles were to avoid loading the bolt from the cartridge output and to have the low-mass retaining cylinders dissipate their energy on impacting together rather than against the housing.

PROCEDURE

The experimental program was divided into six major divisions: establish monitoring apparatus, function the six flight-type separation nuts, analyze the performance records and compare nut performances, determine the housing performances with only a standard bolt (no stud monitor), determine the effects of bolt torque on shock performance, and consider the possible effects on a typical spacecraft system. In the course of this program, 35 separation nuts were functioned; the number and type of nuts tested are summarized in Table I.

Monitoring Apparatus

To evaluate the response and linearity of the monitoring system, the bar was impacted with a steel ball and was used to monitor the noncaptive nut, shown in figure 2. The bar impacts were accomplished by a 0.24-kg (0.54-lb) steel ball, 3.18 cm (1.25 in.) in diameter, on a 152.4-cm (60-in.) pendulum at horizontal displacements of 30.48 cm (12 in.), 60.96 cm (24 in.), and 91.44 cm (36 in.) from the bar's end, at heights of 3.048 cm (1.2 in.), 12.7 cm (5.0 in.), and 30.48 cm (12 in.). Several flat-ended cylindrical and conical adapters were threaded to the bar and impacted with the ball to determine the effect of interfaces and possible internal reflections. All interfaces were coated with silicone grease to maximize shock coupling. The noncaptive nut was torqued to 11.298 Nm (100 in-lb) on the monitoring bar for functioning.

Nut Performance

The six separation nuts were functioned under as nearly identical conditions as possible; each nut was torqued to 11.298 Nm (100 in-lb) on the stud monitoring bar, and the housing flanges (except for Low-Shock Design 4, see Apparatus) were bolted to the housing monitoring bar. Several nuts of each nut type were functioned in this arrangement: Six each of Standard Designs 1 and 2, and six each Low-Shock Designs 1 and 4, and one each of Low-Shock Designs 2 and 3. An effort was made to associate the mechanisms of the functioning with the force-time history obtained from the stud and housing monitoring bars. The motion of the monitoring bars was observed with a 400-pps framing camera to estimate the impulsive loading on functioning. This motion was equated to energy by multiplying the displacement height by the weight of the bars.

Performance Analysis

For comparison the force and acceleration time histories of one representative record of each nut type were plotted on the same scales. Also, the impulsive loads produced by the actuation of each nut type were compared.

The acceleration time histories of the representative records were analyzed on a shock spectrum analog analyzer (MB model 980) to 40 kHz with a Q of 10. Only the first pulse produced by each channel was analyzed and only for the duration of the pulse to produce a primary spectrum; that is, the reflected pulses were disregarded in the analysis, and the spectra produced represent the absolute response of a mass within a single-degree-of-freedom system only within the time period of the pulse itself, a maximum time of 1.34 milliseconds. In like manner, the acceleration response of a single-degree-of-freedom system to the force pulses could be calculated and presented in spectral form.

Stud Performance

To simulate the mounting normally used in separation systems, in which the nut housing is secured to the structure and the stud is allowed to move, five nuts (all except Standard Design 2) were functioned with a free stud and were monitored only on the housing side. The force time histories of the housing were compared to the performance utilizing both monitoring bars. Also, the stud ejection velocities produced on actuation of the nuts were observed with a 400-pps camera. This velocity was related to kinetic energy $1/2\ mV^2$.

Effect of Torque

To determine the effect of torque on shock generation, four additional nuts were functioned at torque levels greater than 11.298 Nm (100 in-lb) (45.194 Nm (400 in-lb) to 101.686 Nm (900 in-lb)) using both bars: Noncaptive nut, Standard Design 1, Low-Shock 1, and Low-Shock 4. Their force time histories were compared to the corresponding tests at 11.298 Nm (100 in-lb).

Effects on Spacecraft

Based on the force time histories produced by these low-shock nuts, the general effect on spacecraft systems was considered. Under consideration were relative shock loads, effects of mounting, and relative displacements on actuation.

RESULTS

Monitoring Apparatus

Several observations can be made from the force and acceleration records obtained from impacting the 3.18-cm (1.25-in.) steel ball against the bar's end shown in figure 9. There is a 1.34-millisecond period from the beginning of the initial compression wave, until the arrival of the reflected wave which is first tensile, then compressive. According to theory, the acceleration is proportional to the first derivative of the force signal. Consequently, if the input force pulse is not a true sine wave, the derivative will be a complex wave, requiring up to twice the input's frequency to reproduce. In the examples in figure 9, the input force is evidently a haversine pulse, since the acceleration pulse indicates two acceleration peaks, producing a pulse that is equivalent to twice the frequency of the input pulse. Also, since the accelerometer is mounted on the bar's end, the acceleration is twice the level that would be recorded at a point along the bar. The amplitudes of these simple impact-generated pulses provide a basis of comparison for the loads induced by the function of the separation nuts; that is, at a 91.44-cm (36-in.) displacement the impact velocity of the steel ball is 4.24 m/sec (13.9 ft/sec), producing a 11.076-kN (2490-lb) force, 118-microsecond pulse.

No appreciable losses nor internal reflections were produced by the straight cylindrical adapters; this was also observed for a 45° expansion conical adapter (from 2.54 cm (1 in.) to 5.08 cm (2 in.) diameter, the angle used in the housing adapter).

Typical performance plots for the noncaptive nut are shown in figure 10. The initial tensile pulse is produced by the force required to shear a pin at the retaining ring to collet interface and to overcome friction. (See cross section, fig. 2.) The pressure within the cavity then loads the stud into compression until the stud is released. The oscillating acceleration pulse bears little visual correlation to the input force pulse. The impulsive load on the stud caused the monitoring bar to swing approximately 25.4 cm (10 in.), equivalent to 2.99 Nm (26.5 in-lb) of energy. The remaining energy in the nut housing was not recorded.

Separation Nuts

The functional performance of each nut type will be explained individually in this section through representative performance curves. In general, the performances produced by several units of each type of nut were highly repro-

ducible. The performance curves could be exactly overlaid from nut to nut with only small variations in amplitude.

Standard Design 1.- See figure 3 for the cross section and figure 11 for the functional histories. As the retaining cylinder is forced to the right, a momentary tensile wave is created in the bolt. This is followed by a strong compressive force produced by the piston against the collet. The major tensile spike is produced by the retaining cylinder stroking the flared portion of the collet. The housing first experiences a tensile wave as a reaction force to the acceleration of the retaining cylinder applied through the collet. As the retaining cylinder impacts against the O-ring and housing, a strong compressive pulse is produced. The monitoring bars were observed to swing apart by approximately 15.24 cm (6 in.) on functioning.

Standard Design 2.- See figure 4 for the cross section and figure 12 for the functional histories. The initial tensile load in the stud appears to be produced by the housing reaction in loading through the collet which exceeds the compressive loading produced by shearing the shear pin between the retaining cylinder and the collet. The large compressive spike is produced by the impacting of the retaining cylinder, bottoming against the housing. The housing load first exhibits a compression corresponding to the reaction to the initial tensile load of the stud. The major shock of the impacting retaining cylinder is apparently transferred efficiently into the stud mass and not the housing. The second compressive load of the housing can be attributed to the bottoming of the spring or spreader piston against the retaining cylinder in ejecting the stud. The positive pulse could be related to the seating of the spreader piston in the then-expanded collet sections. The monitoring bars swung apart approximately 20.32 cm (8 in.) on functioning.

Low-Shock Design 1.- See figure 5 for the cross section and figure 13 for the functional histories. The initial tensile pulses on the stud can be related again to the shearing of a shear pin and friction when the retaining cylinder begins its motion. The major compressive indication is caused by the loading through the pistons and honeycomb. The retaining cylinder impacting the flared portion of the collet produces the sharp tensile pulse. The loads into the housing are apparently well isolated from the stud; the reactionary forces are low, reduced by the crushable honeycomb and the acceleration of the high-mass piston. A small tensile load is coupled through the washer at the interface, followed by a compression produced by decelerating the retaining cylinder against the housing. No separation of the bars was observed on functioning.

Low-Shock Design 2.- See figure 6 for the cross section and figure 14 for the functional histories. The initial stud compressive load is produced by the force of the spreader piston on the collet on pressurization. The tensile pulse is produced by the friction of the retaining cylinder withdrawing over the collet. The subsequent compressive pulses are then created by the piston-loaded segments sliding outward and bottoming into the cavity to release the bolt. The stud is abruptly off-loaded when the piston is stroked to the right by the internal shoulder of the retainer cylinder. The housing experiences the small compressive pulse due to a pressurization force to the right, followed by the tensile pulse produced by the reaction to the friction resistance in forcing the retaining cylinder to the right. The next compressive pulse is the reac-

tion to the loading of the collet by the piston. The remaining compressive pulse can be attributed to the deceleration of the retaining cylinder and piston within the housing by the residual gas from the cartridge. The bars swung apart approximately 10.16 cm (4 in.) on functioning.

Low-Shock Design 3.- See figure 7 for the cross section and figure 15 for the functional histories. The initial tensile indication on the stud is due to the movement of the retaining cylinder to the right. The hinging piston applies the major compressive load, which is quickly converted to tension when the retaining cylinder's recessed area impacts the projection of the collet. The second compressive pulse can be attributed to the forcing of the combination of hinging piston, retaining cylinder, and collet to the left, and applying a compressive load against the stud. The initial tensile load produced by the housing can be atrributed to the reaction to the retaining cylinder's motion to the right. The compressive pulse is the reaction to the loading of the collet. On release of the bolt, the housing load would remain compressive during the deceleration and reversal of the piston/cylinder. A positive pulse would be produced on the impacting of the piston/cylinder against the bottom of the housing. The bars were observed to swing apart approximately 20.32 cm (8 in.) on functioning.

Low-Shock Design 4.- See figure 8 for the cross section and figure 16 for the functional histories. The loads by the converging retaining cylinders coupled into the collet, and transferred into the stud, are essentially balanced. The compressive load may be attributable to the relaxation of the long-length stud on release. The major identifiable load produced by the housing is compressive, possibly caused by a pressurization of the port volumes. The force is appreciably higher as compared to the other nuts, due to the mounting of the bar into the nut cap rather than in a flange at its base. No separation motion of the monitoring bars was observed.

Performance Analysis

The functional performance comparisons are shown in figures 17 to 19. The shock spectral analyses are shown in figures 20 and 21.

The stud force and acceleration levels of the low-shock designs, as shown in figure 17, are appreciably lower than the levels produced by the standard designs. The contrasts in force levels are not reflected in the acceleration comparisons. The housing loads, shown in figure 18, of the low-shock designs are lower than for the standard units except for Low-Shock Design 3. However, the acceleration levels of the low-shock designs were considerably lower as shown in figure 19.

The impulsive loading performance for each nut type is compiled in table II. The highest impulse was produced by the noncaptive nut, since a single 14.33-kg (31.6-lb) bar was swung 25.4 cm (10 in.) (a height change of 2.13 cm (0.84 in.)). The impulse produced by the remaining nuts was delivered to two bars, producing considerably less height change. The total impulse delivered by the nuts can be directly related to the integral of the force-time curves delivered into each bar. Although the peak stud loads of Standard Design 2 are more than 16 times those of Low-Shock Design 3, the total impulsive loads are the same. Obviously,

the least-shock-producing method of delivering an impulse to achieve a desired separation of interfaces is to apply lower level loads over a longer time interval.

The stud performance spectra in figure 20 indicate that energy levels are present to 40 kHz. The highest response was produced by Standard Design 2, particularly at high frequencies. The lowest response was produced by Low-Shock Design 4 whose primary content is above 4 kHz.

The housing performance spectra (fig. 21) are not so clearly differentiated as the stud performance (fig. 20). The acceleration spectra indicate Low-Shock Design 1 to produce the highest levels at frequencies to 1000 Hz.

Stud Performance

The force performances of the five separation nuts using a free stud, compared to using a two-bar monitoring system, are shown in figures 22 to 26.

The initial tensile loads, produced by pressurization of the nut body and the forces necessary to overcome friction in the retaining cylinder withdrawal, were considerably increased for all nuts; the increases ranged from two to six times the loads observed in the two-bar system. Although the amplitudes were higher, the performance histories from the free-stud functionings are very similar to the performances from the two-bar systems.

The secondary loads of Standard Design 1 and Low-Shock Designs 1 and 4 produced by the actuation of separation mechanisms or decelerating masses were appreciably increased. However, the secondary loads produced by Low-Shock Designs 2 and 3 in the free-stud setup, although somewhat different in shape, were essentially the same as for the two-bar system.

The force-performance differences and similarities can be attributed to the manner in which the nuts' internal components couple loads to the surrounding structure and dissipate their energy. The increased loads were caused by a lack of coupling into the stud monitoring bar. The lack of increased loads indicates that the mechanisms of internal energy dissipation were not appreciably changed.

The velocities of the studs achieved on functioning the nuts varied from zero to 2.80 m/sec (9.2 ft/sec) and are shown in table II.

Effect of Torque

The force-performance histories of the four separation nuts torqued to higher levels are shown in figures 27 to 30. The performances of the noncaptive nut, Standard Design 1, and Low-Shock Design 1 are essentially the same within normal functional variations. However, the loads in the Low-Shock Design 4 were considerably increased. Since the only force required to achieve separation in Low-Shock Design 4 is that of moving the small-mass retaining

cylinders, an increase in friction caused by an increase in torque level would significantly affect the force to initiate and stop this motion.

Effects on Spacecraft

This study has produced several significant points of information for consideration by a spacecraft systems designer in the application of pyrotechnic separation nuts.

Pyrotechnic separation nuts can be produced that generate low-shock outputs on functioning. The low-shock nuts evaluated in this study are in various stages of development and have yet to be applied to any aerospace program. Some penalties may be introduced in these low-shock nut designs in increased weight, volume, and complexity of the release mechanism over the existing commonly used pyrotechnic separation nuts. Also, each of the nuts can be designed to contain two gas-generating cartridges as an approach to redundancy. Should both cartridges be functioned simultaneously to achieve actuation, considerably higher shock loads would be produced, since internal pressures could be doubled, yielding considerably higher forces. To maintain minimal shock loading, the second cartridge should be functioned only if the first failed to achieve separation. Further, care should be taken to avoid sympathetic ignition between cartridges; that is, the second cartridge should be sufficiently protected to prevent ignition by the hot gases produced by the first cartridge.

Due to relative loads induced into the stud and housing on actuation of these low-shock nuts, some decisions should be made on physical mounting and attachment. Peak shock loads are reduced significantly on nut actuation by providing maximum coupling of loads to structure on both sides of the separations plane; that is, with the housing and stud rigidly attached to the structure. Shock loads are increased in the nut housing by a freely moving stud. Little or no impulsive loading is introduced into a rigidly mounted stud by Low-Shock Designs 1 and 4 to accomplish separation. The impulsive loads in Low-Shock Designs 3 and 4 are insufficient to eject a stud that is free to move. The impulsive loads produced by the remaining nut designs can produce a desired separation of structure or stud ejection in a well-controlled manner. Also, lower-level shock loads are introduced into the stud side of the separation plane, as compared to the housing side, for Low-Shock Designs 3 and 4. The reverse is true for Low-Shock Designs 1 and 2. Finally, only Low-Shock Design 4 of the four tested (noncaptive, Standard 1, Low-Shock 1 and 4) exhibited any increase in shock levels due to an increase in torque level of the mounting stud.

Although the peak shock loads of the complex high-frequency pulses produced by these low-shock nuts are considerably less than for the standard designs, the question still remains as to what part of a spacecraft is affected, and to what degree. These shock loads are well below the elastic limit of metals and should have little effect on primary structure. The total impulsive load is small, since the pulse width is generally 1 millisecond or less. However, high-frequency shock loading of small-mass, flexible items, such as electronics, can produce significant effects. The high-frequency content of these pulses can be significantly decoupled and amplitudes lowered by interfaces, bolted or riveted joints, and low-density mounting pads on the electronic chassis, according to

current investigations accomplished by the Viking Project Office (NASA Langley Research Center). Experiments to investigate shock isolation of the nut body and interfaces have been unsuccessful, since the use of low-density materials prevents adequate mechanical linkage.

The dynamic analysis of spacecraft structure can be appreciably enhanced through the use of actual force time histories as well as through the current practice of using acceleration histories. However, the theoretical prediction of dynamic response of spacecraft to these high-frequency inputs is still a difficult problem area, because of the limitations of most computer programs for structural analysis. Spectral analyses of acceleration pulses do not compensate for phase and time relationships. The integration of acceleration signals to produce more useful force signals is difficult to accomplish electronically. Also, the dynamic response of strain-gage monitors is considerably better than that of acceleration monitors for this high-frequency environment. Finally, strain gages can be directly attached to a structure without modifying the structure or significantly increasing the mass of the structure as compared with the use of accelerometers.

CONCLUSIONS

The conclusions drawn from this study can be categorized into three areas: low-shock separation nuts, their relative effect on a spacecraft system, and monitoring systems.

Pyrotechnic separation nuts that generate a low mechanical shock on actuation can be produced. Four different separation nut designs were evaluated in this study, demonstrating a reduction in shock forces by factors from 10 to 100, as compared to a commonly used pyrotechnic separation nut. However, some penalties may be introduced in increased volume, weight, or complexity. The performance and physical characteristics of each nut are unique, each having its own advantages and disadvantages. Examples are: One type produces no separation forces but has a high weight; another produces low impulsive loads into a fixed stud but requires an increase in volume to function; and a third produces low impulse into a free stud but produces a higher level shock pulse. The selection of a particular nut on a spacecraft system must be predicted on the system-unique requirements.

To minimize the effects of the functioning of these nuts on the spacecraft system, their location and how they are installed should be predicated on the performances described above. Although the peak shock levels have been significantly reduced over commonly used designs, the short-duration, high-level, high-frequency shock pulse still remains complex. The shock output should have little or no influence on primary structure, but the effect on electronics or flexible components remains unknown. Fortunately, these high-frequency pulses can be effectively attenuated or reflected through the use of interfaces and low-density isolation materials.

The use of strain-gage monitoring systems offers several advantages over the use of conventional acceleration monitoring techniques. Strain gages can

monitor the shock pulses more accurately, have less effect on the structure, and produce information that is more useful for structural analyses than do accelerometers. However, this is not a recommendation to exclude the use of accelerometers. Within the limitations of accelerometers, the data produced are complementary to that produced by strain gages, particularly in complex structures. The simplified-structure monitoring system used in this study has been demonstrated to be an accurate performance-comparison technique for separation nuts. The performance data can be related to actual spacecraft systems.

TABLE I.- NUMBER AND TYPE OF NUTS TESTED PER CATEGORY

Nut type	Performance comparisons	Stud performance	Torque effect
Standard Design 1	6	1	1
Standard Design 2	6		
Low-Shock Design 1	6	1	1
Low-Shock Design 2	1	1	
Low-Shock Design 3	1	1	
Low-Shock Design 4	6	1	1
Noncaptive nut			1

TABLE II.- IMPULSE PERFORMANCE COMPARISONS

Nut type	Two-bar system		Single-bar, free-stud system	
	Displacement, cm (in.)	Energy, Nm (in-lb)	Ejection velocity, m/sec (ft/sec)	Energy, Nm (in-lb)
Noncaptive	*25.4 (10)	2.99 (26.5)		
Standard Design 1	15.24 (6)	.27 (2.4)	2.80 (9.2)	0.136 (1.2)
Standard Design 2	20.32 (8)	.47 (4.2)		
Low-Shock Design 1	None	None	1.34 (4.4)	.031 (.27)
Low-Shock Design 2	10.16 (4)	.12 (1.1)	2.07 (6.8)	.073 (.65)
Low-Shock Design 3	20.32 (8)	.47 (4.2)	**1.27 (.5) motion	None
Low-Shock Design 4	None	None	**.635 (.25) motion	None

*Single-bar displacement.
**Not ejected.

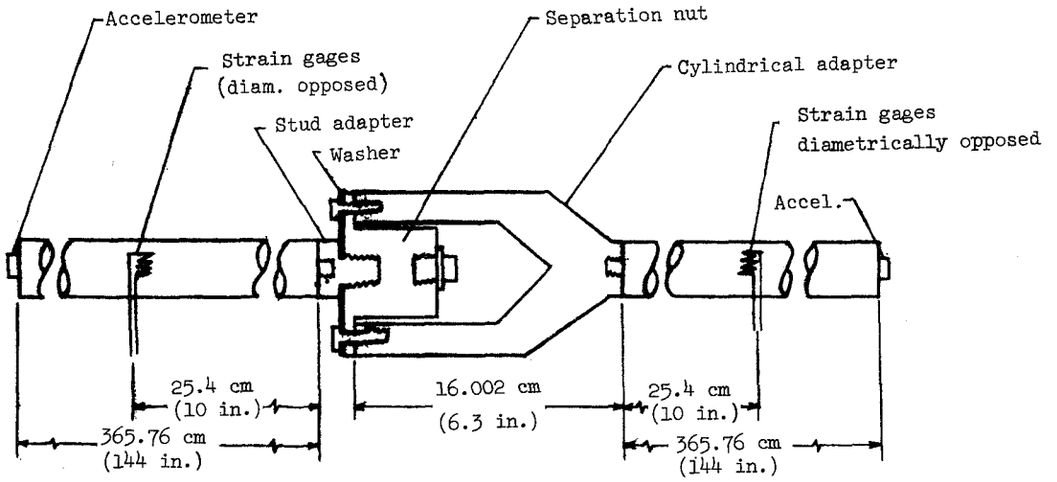

Figure 1.- Cross section of shock monitoring apparatus.

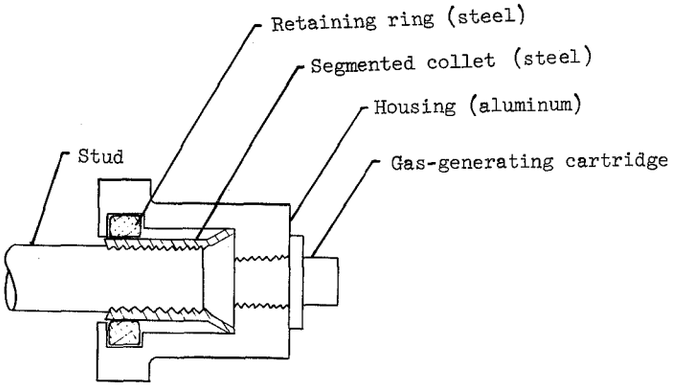

Figure 2.- Cross section of noncaptive separation nut.

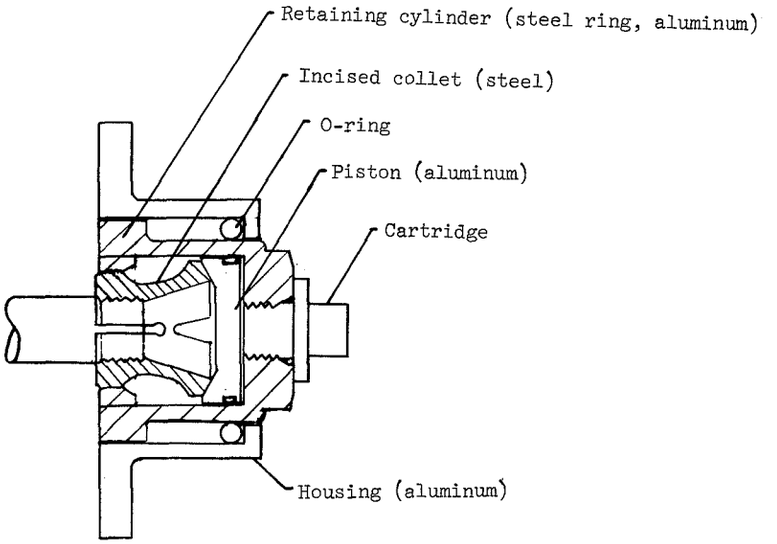

Figure 3.- Cross section of Standard Design 1.

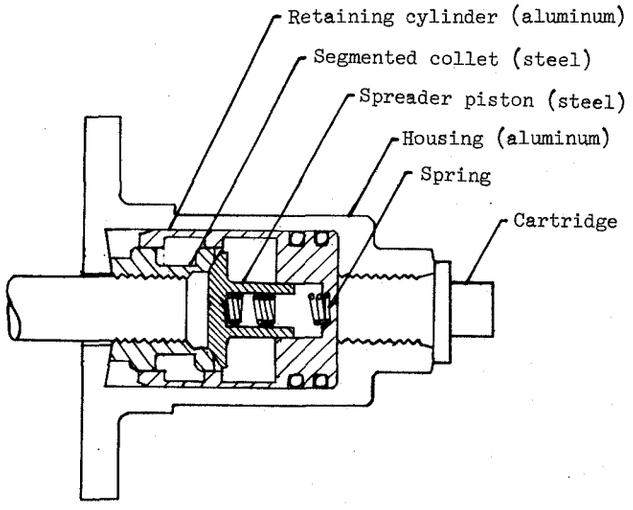

Figure 4.- Cross section of Standard Design 2.

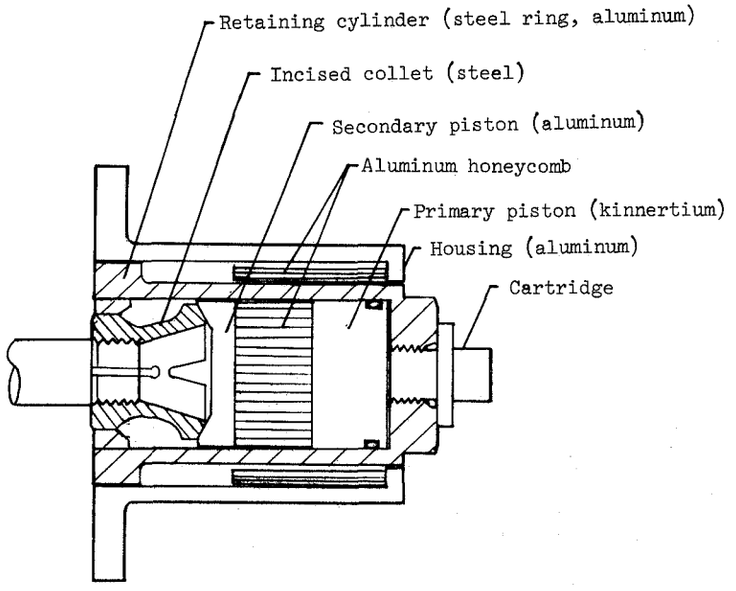

Figure 5.- Cross section of Low-Shock Design 1.

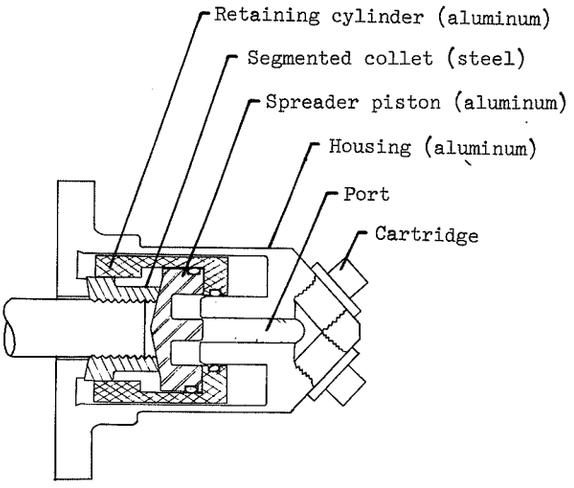

Figure 6.- Cross section of Low-Shock Design 2.

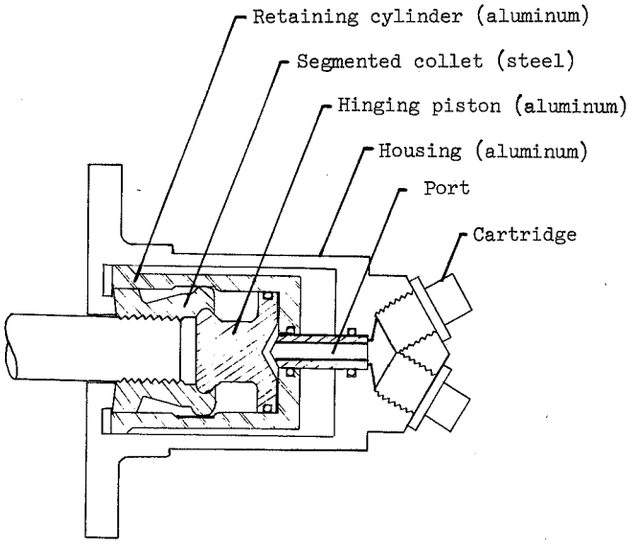

Figure 7.- Cross section of Low-Shock Design 3.

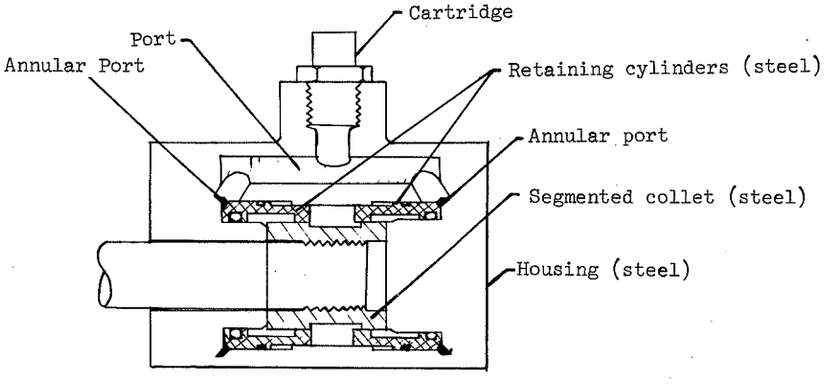

Figure 8.- Cross section of Low-Shock Design 4.

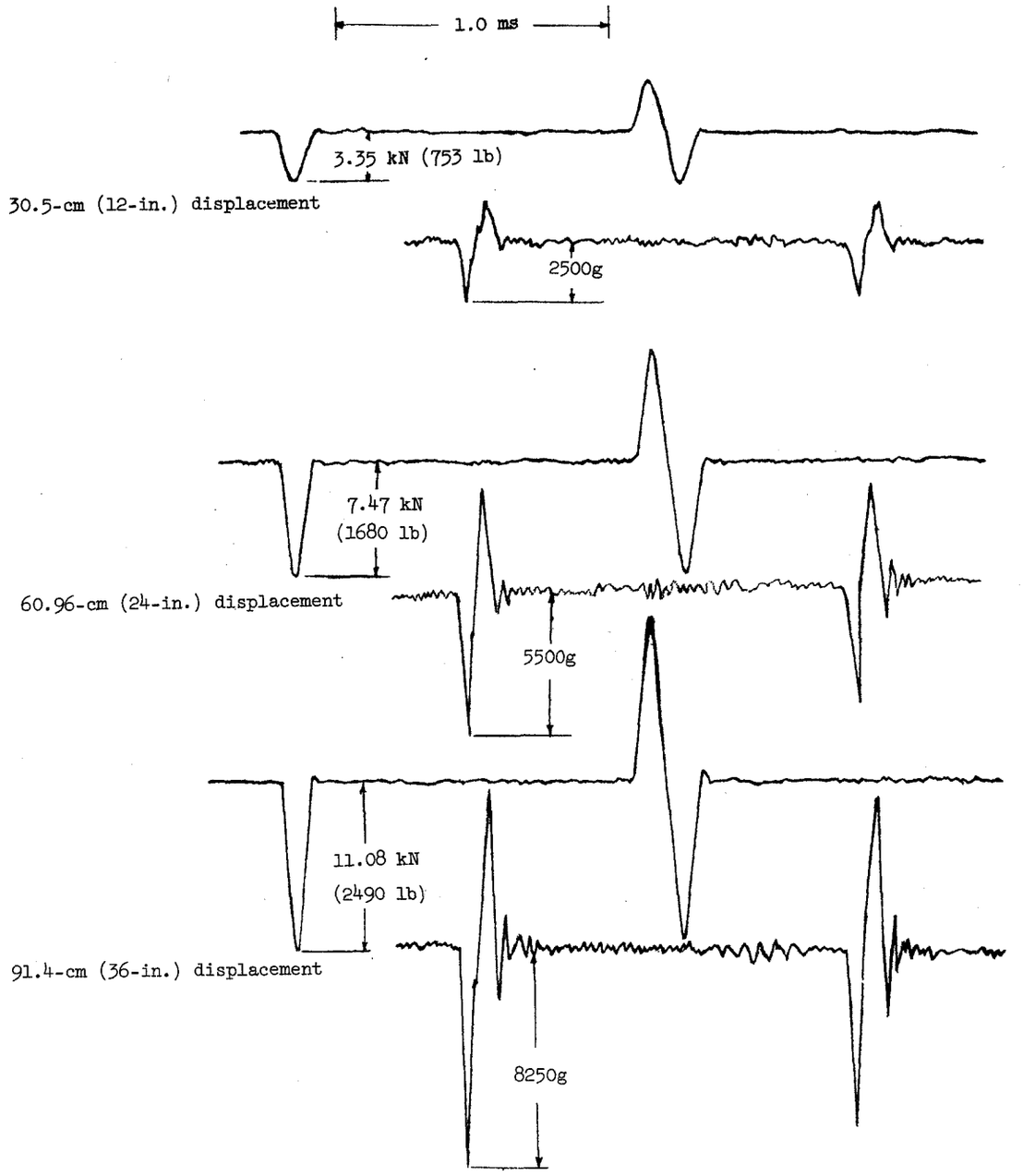

Figure 9.- Force and acceleration performance of 3.18-cm (1.25-in.) steel ball; impacts at horizontal displacements indicated. (1g = 9.807 m/sec^2.)

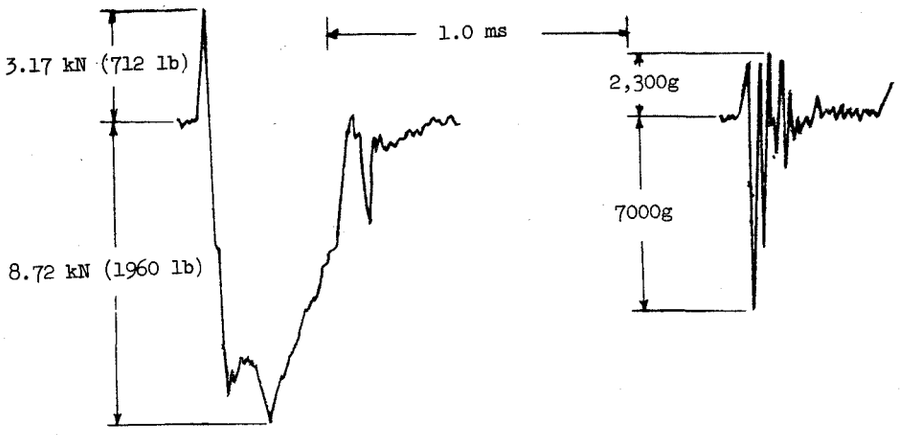

Figure 10.- Force and acceleration performance of noncaptive nut.

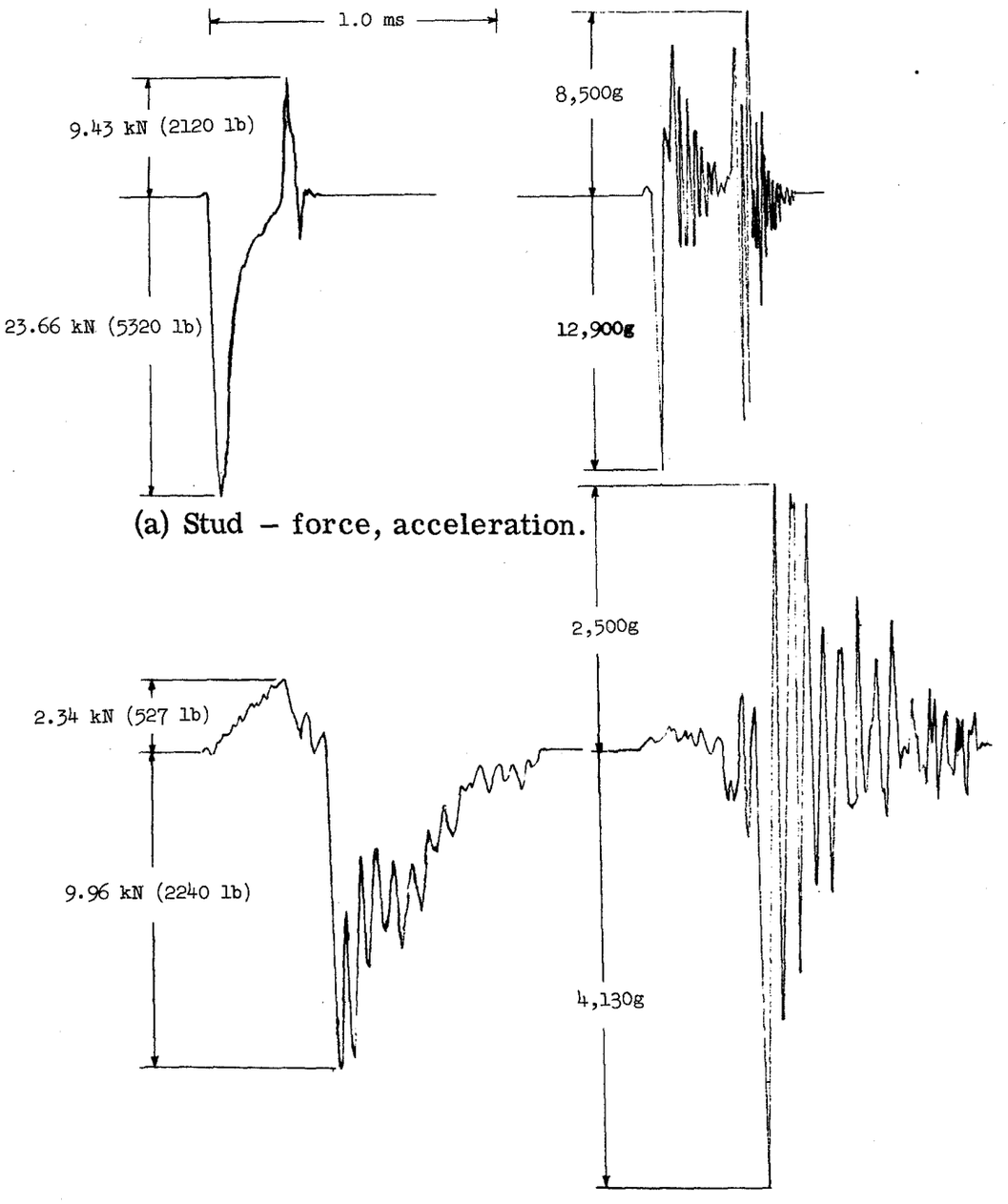

(a) Stud – force, acceleration.

(b) Housing – force, acceleration.

Figure 11.- Force and acceleration performance of Standard Design 1.

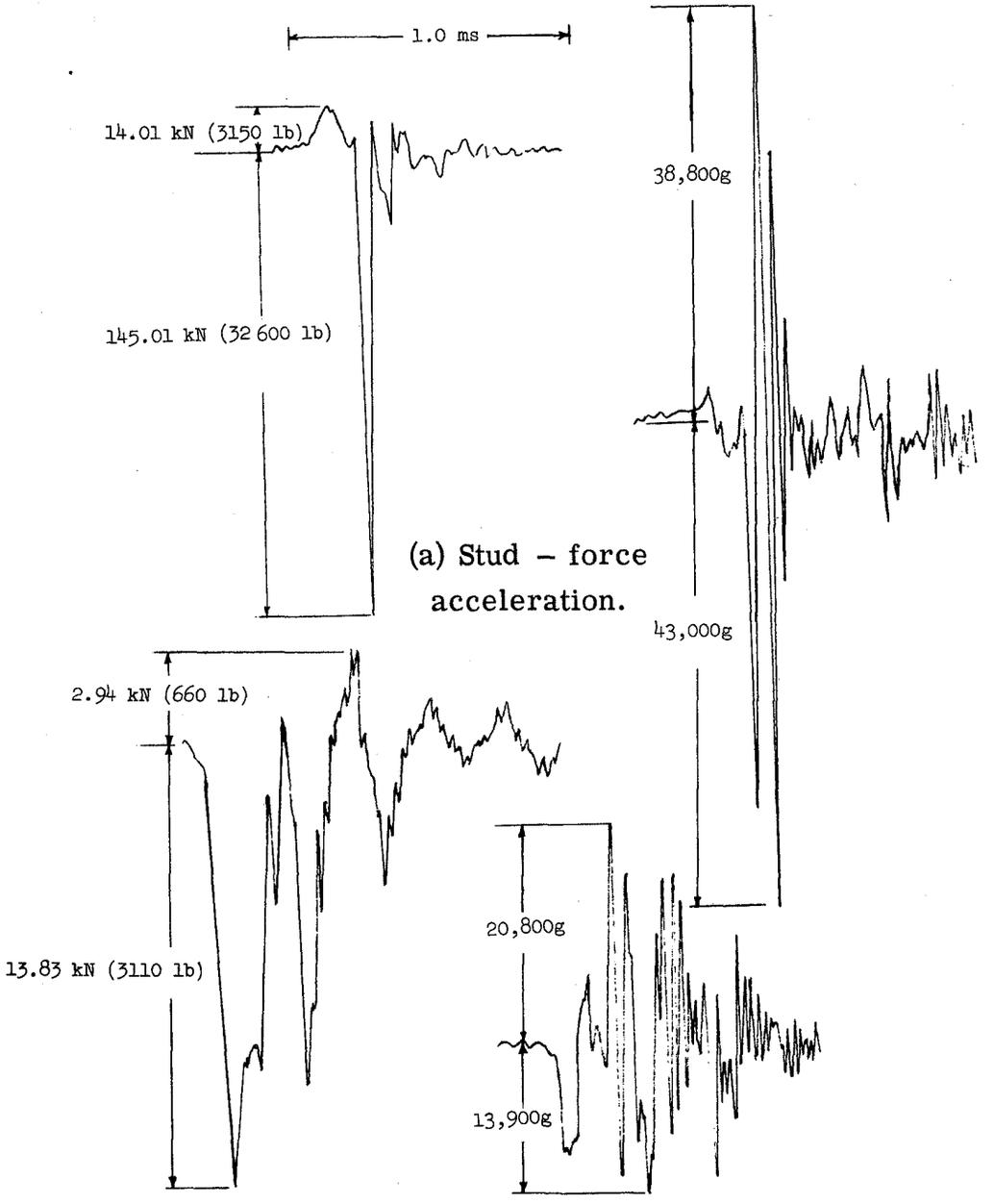

(b) Housing – force, acceleration.

Figure 12.- Force and acceleration performance of Standard Design 2.

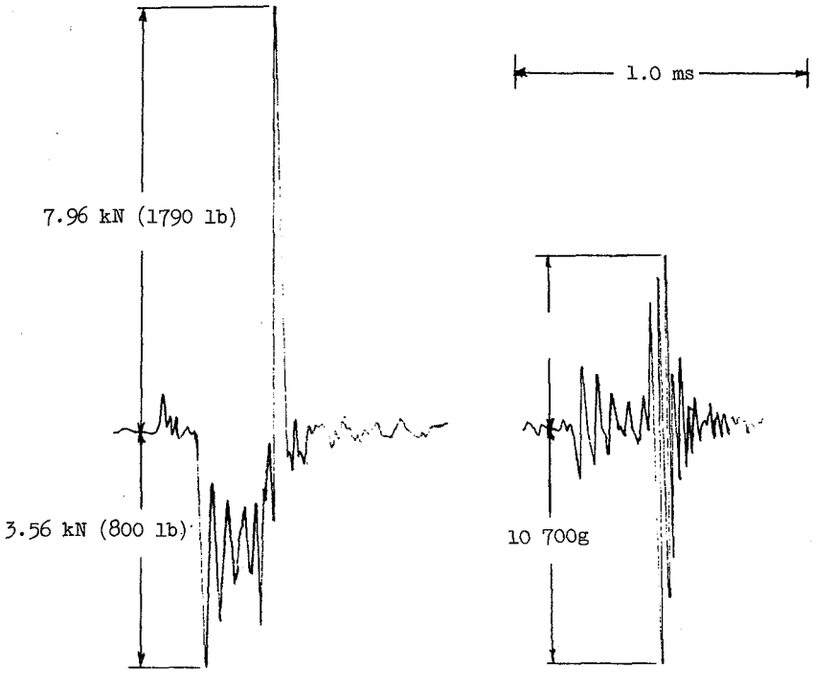

(a) Stud – force, acceleration.

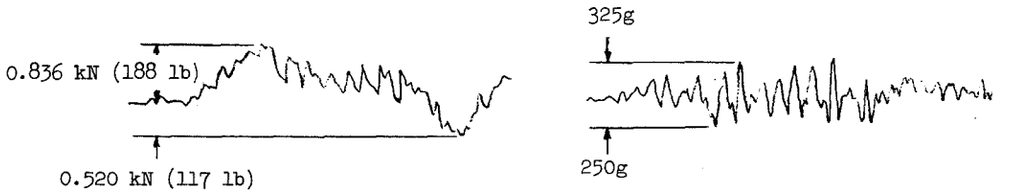

(b) Housing – force, acceleration.

Figure 13.- Force and acceleration performance of Low-Shock Design 1.

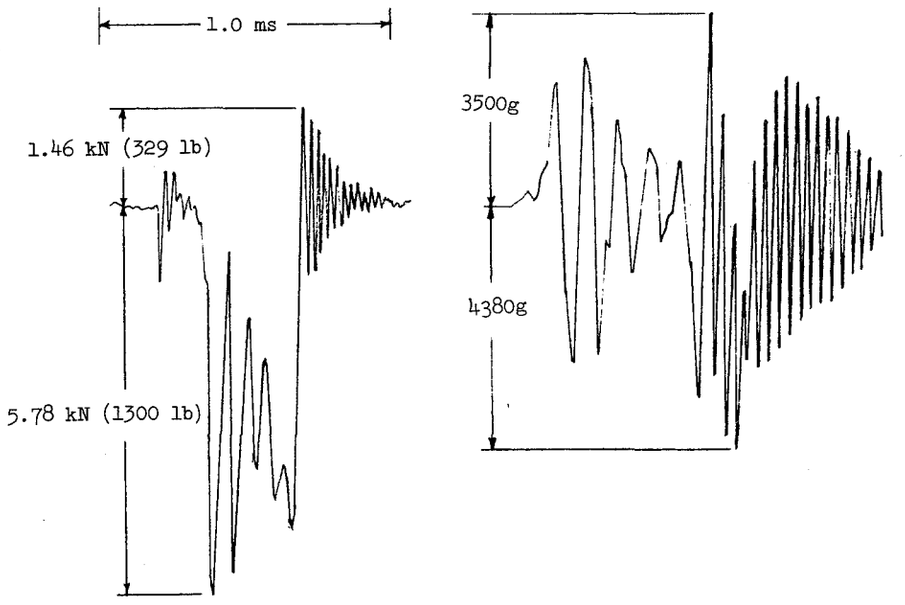

(a) Stud – force, acceleration.

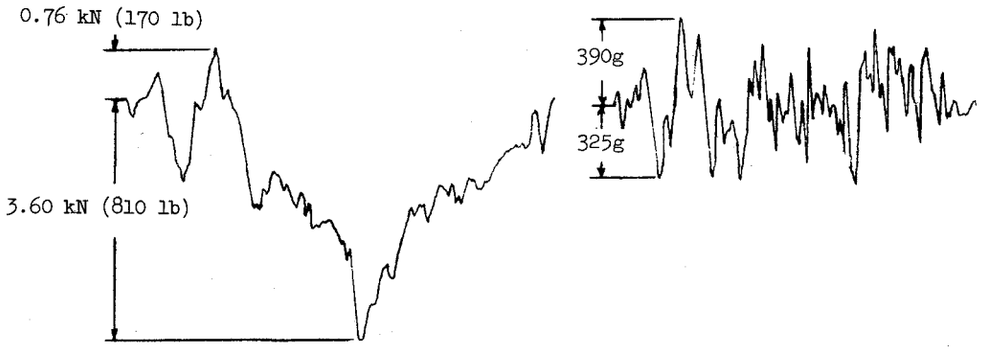

(b) Housing – force, acceleration.

Figure 14.- Force and acceleration performance of Low-Shock Design 2.

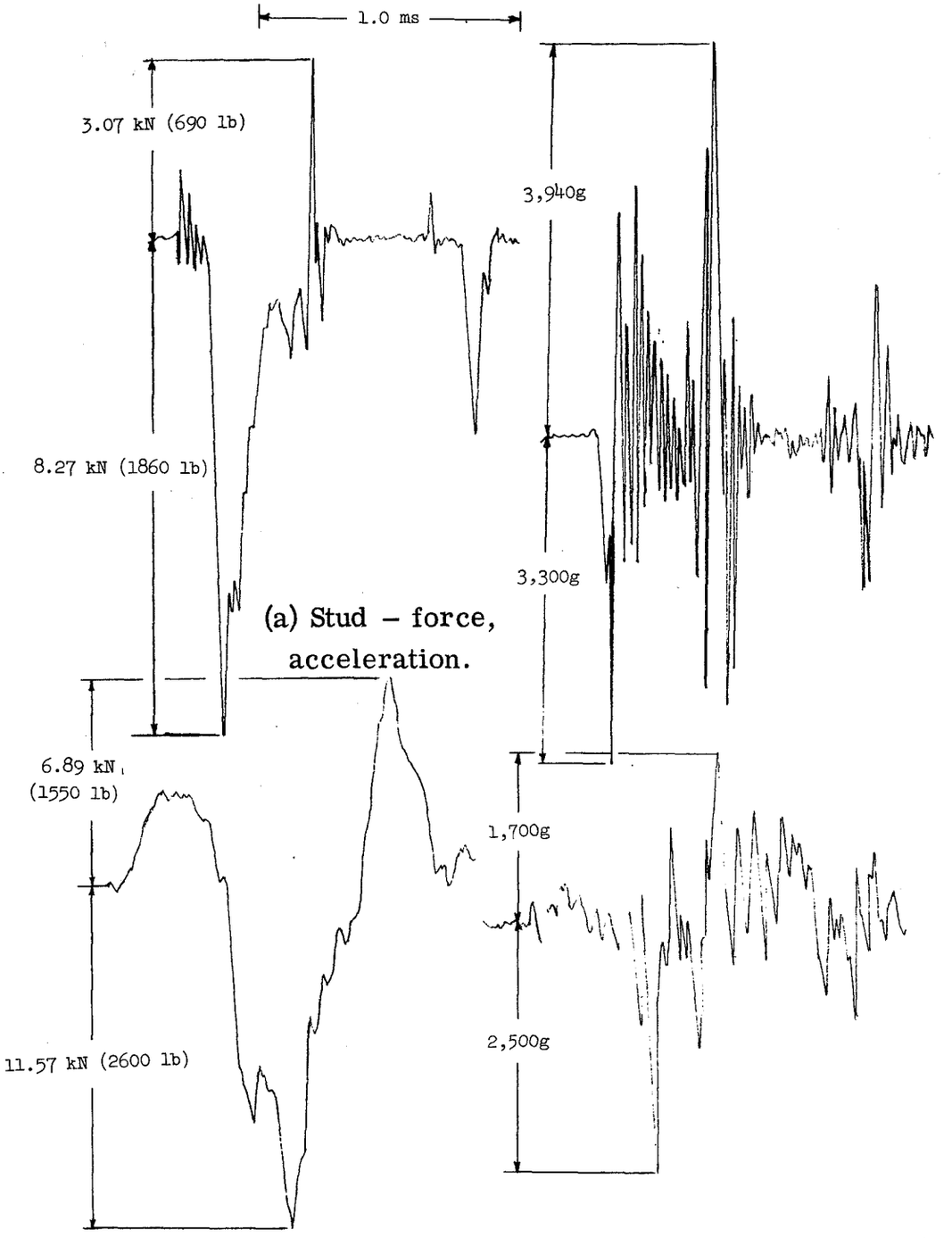

(a) Stud – force, acceleration.

(b) Housing – force, acceleration.

Figure 15.- Force and acceleration performance of Low-Shock Design 3.

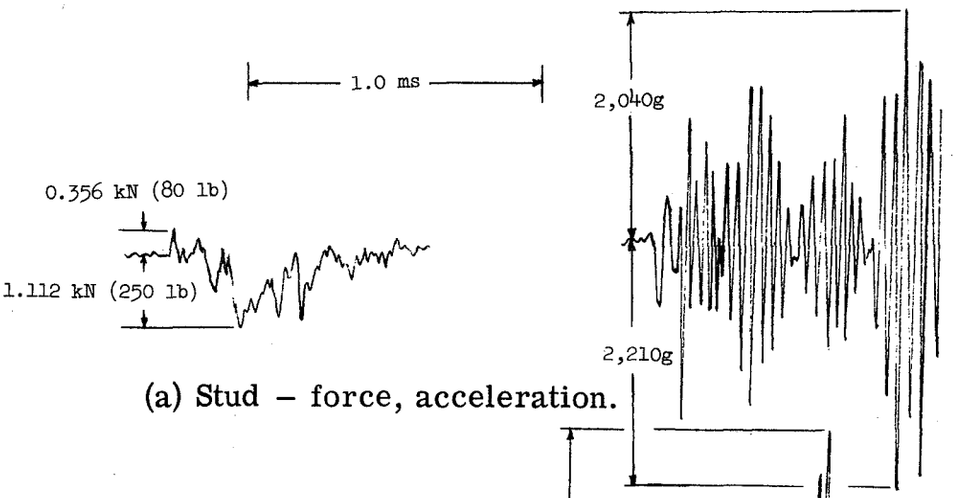

(a) Stud – force, acceleration.

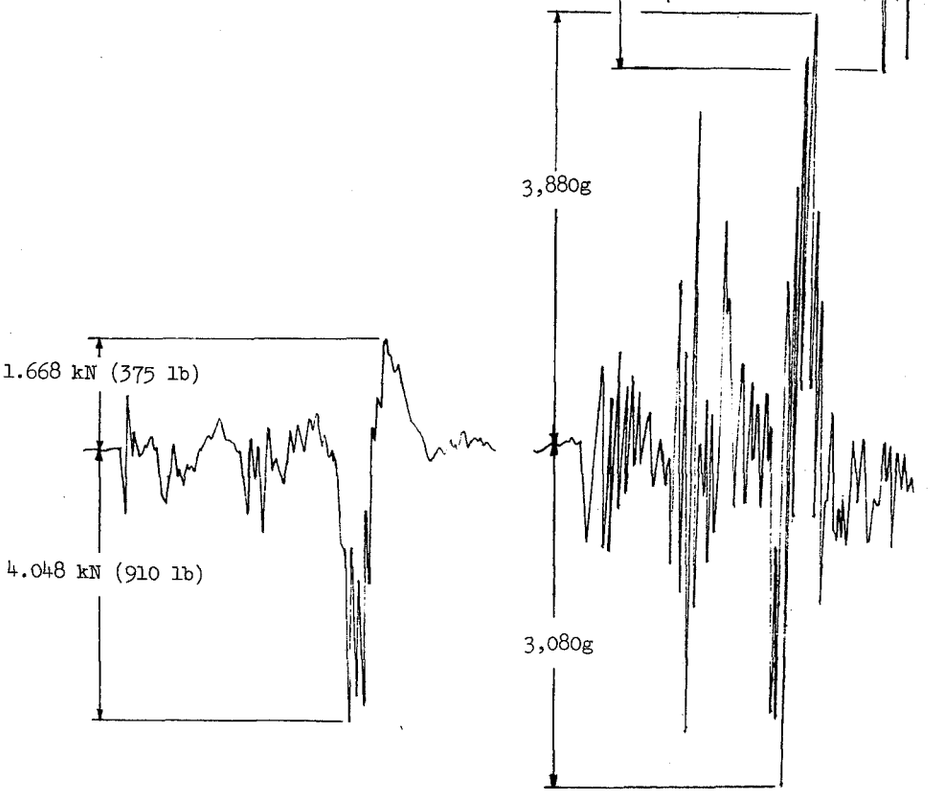

(b) Housing – force, acceleration.

Figure 16.- Force and acceleration performance of Low-Shock Design 4.

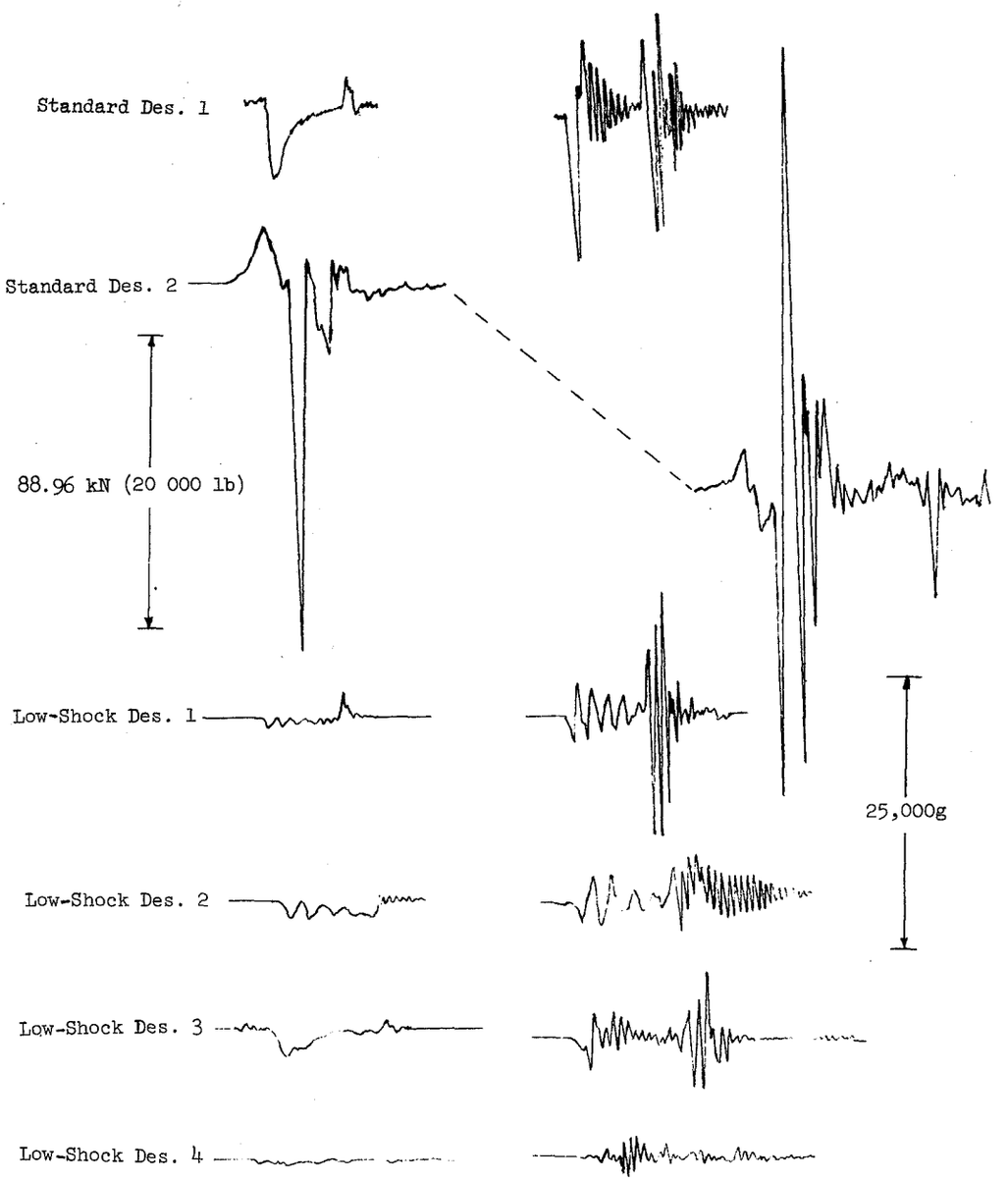

Figure 17.- Stud force and acceleration performance comparison of six separation nuts.

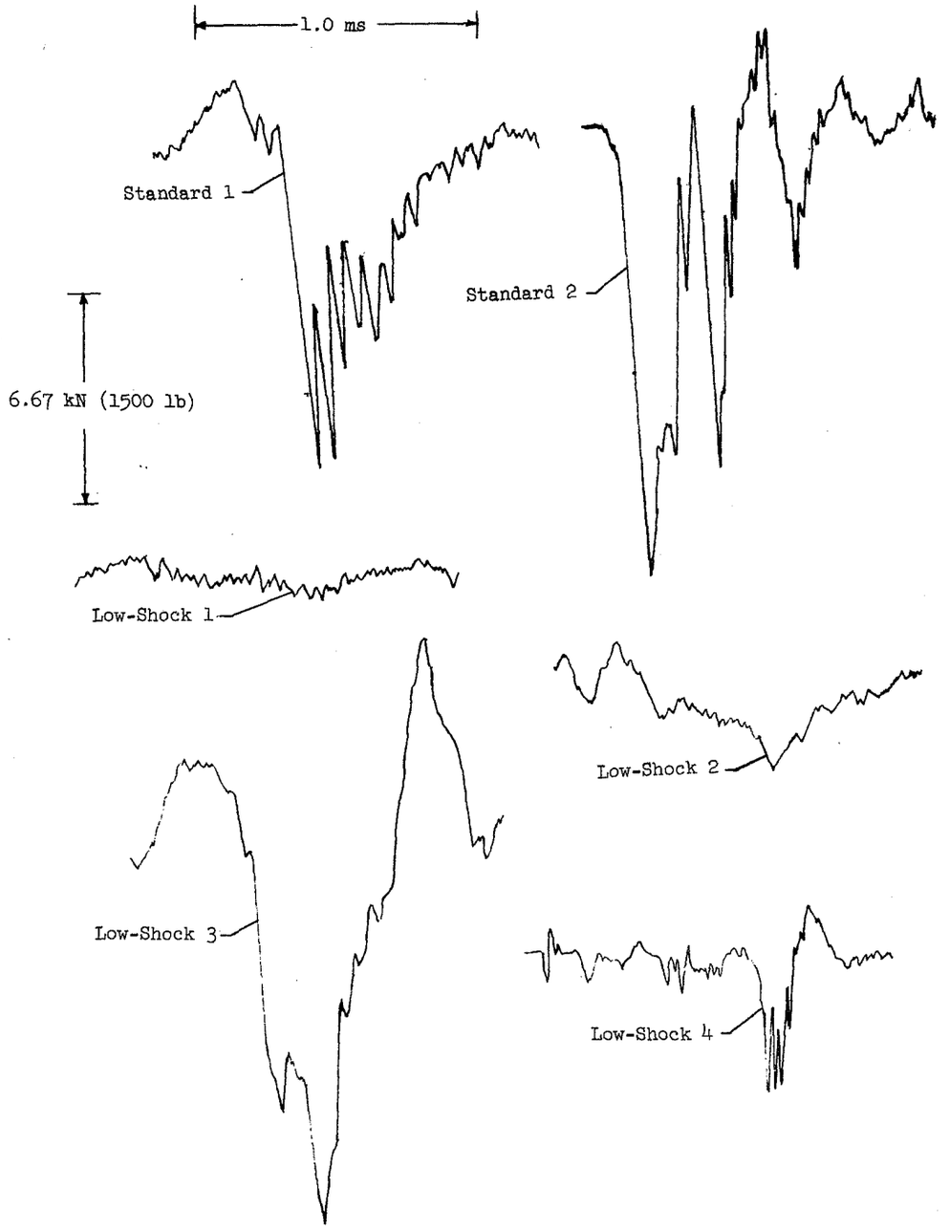

Figure 18.- Housing force comparison of six separation nuts.

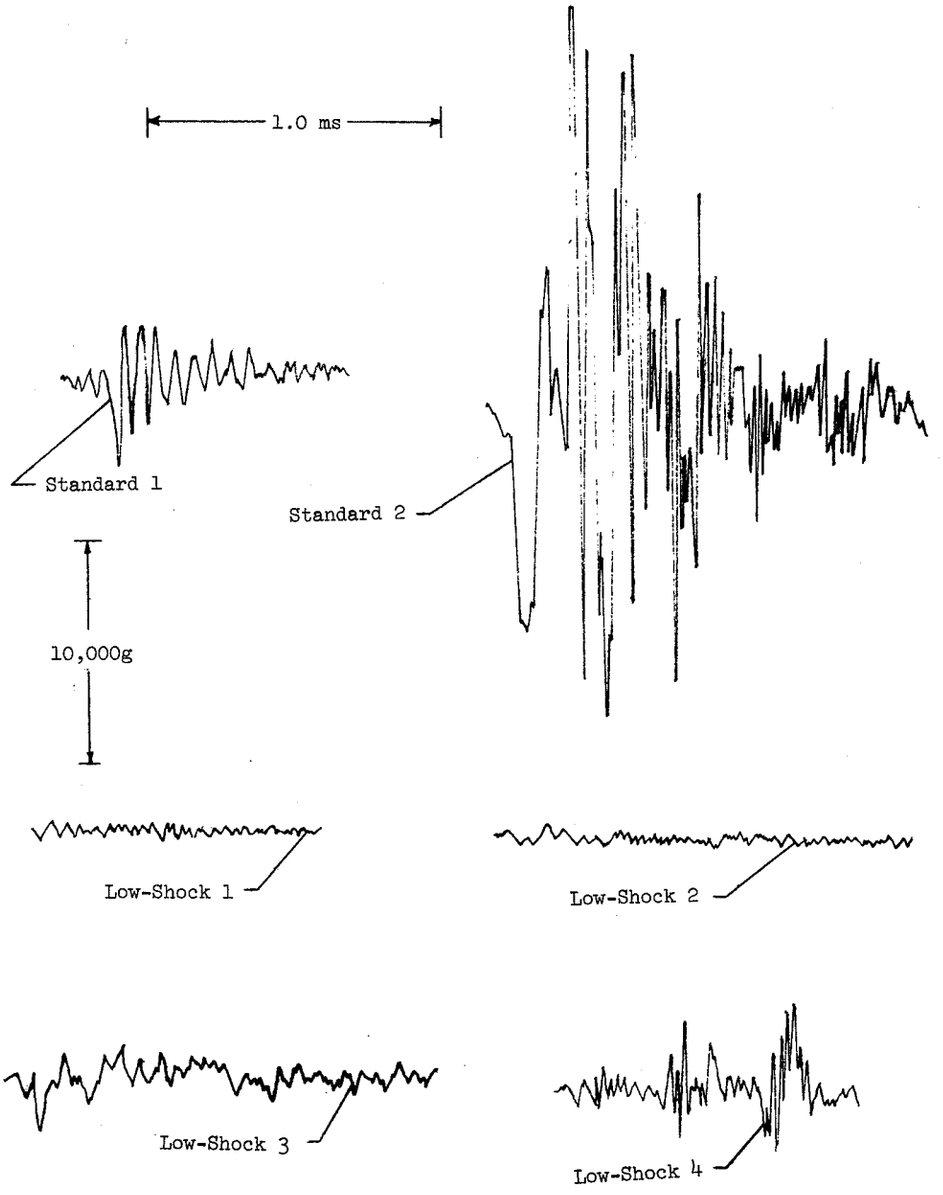

Figure 19.- Housing acceleration comparison of six separation nuts.

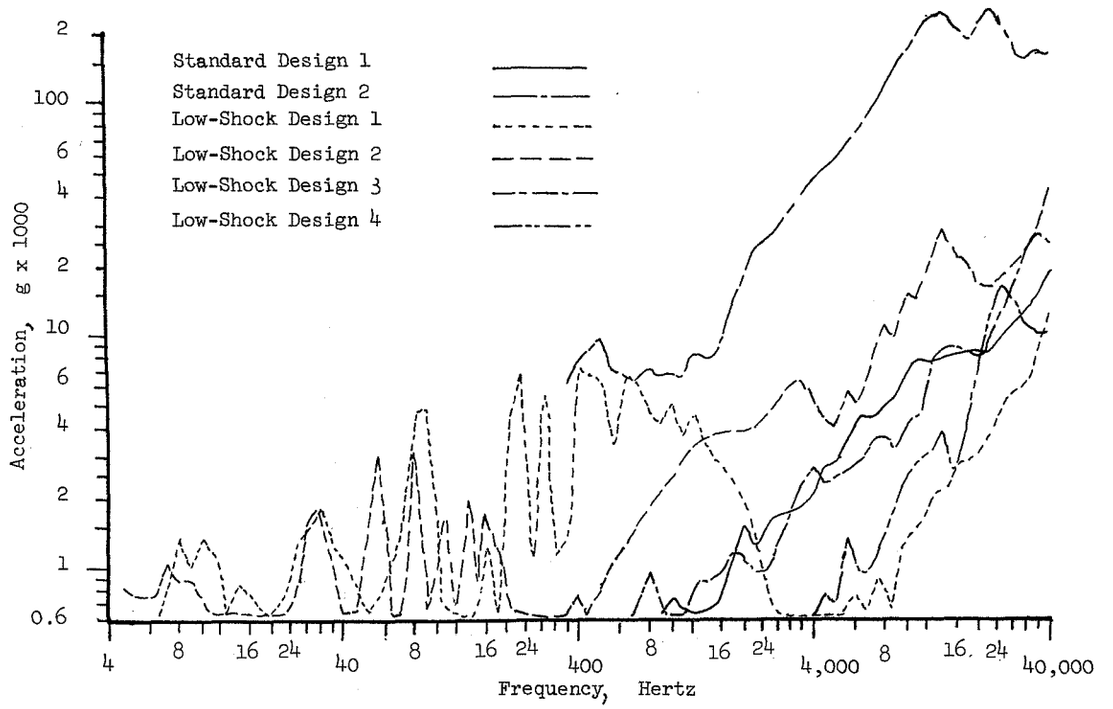

Figure 20.- Stud performance spectra comparison.

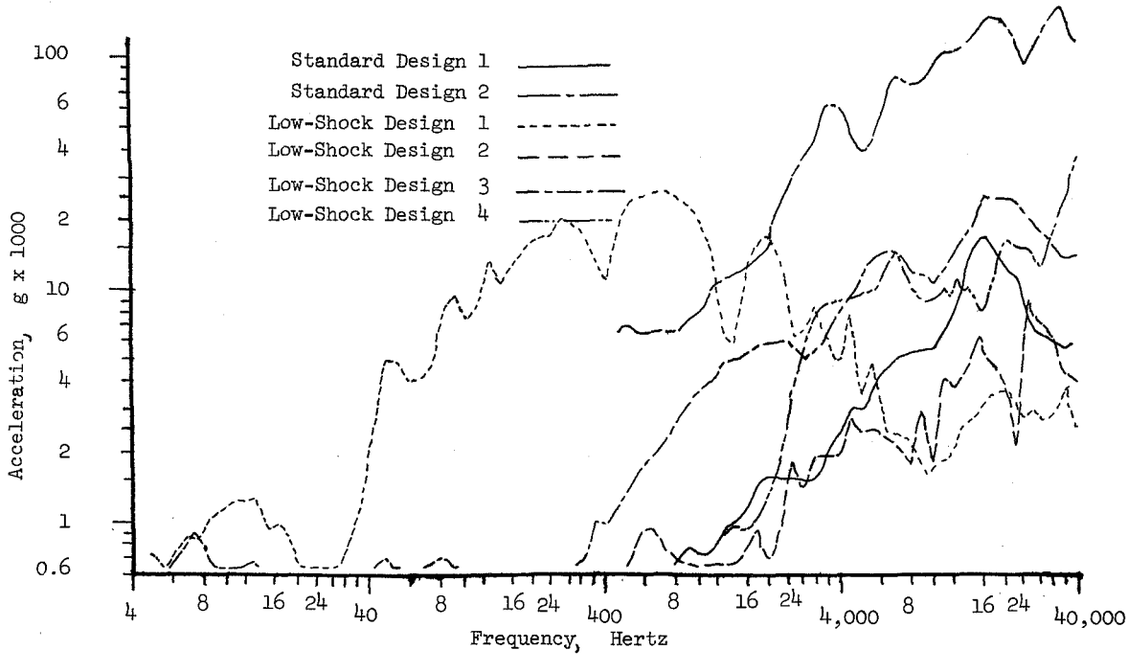

Figure 21.- Housing performance spectra.

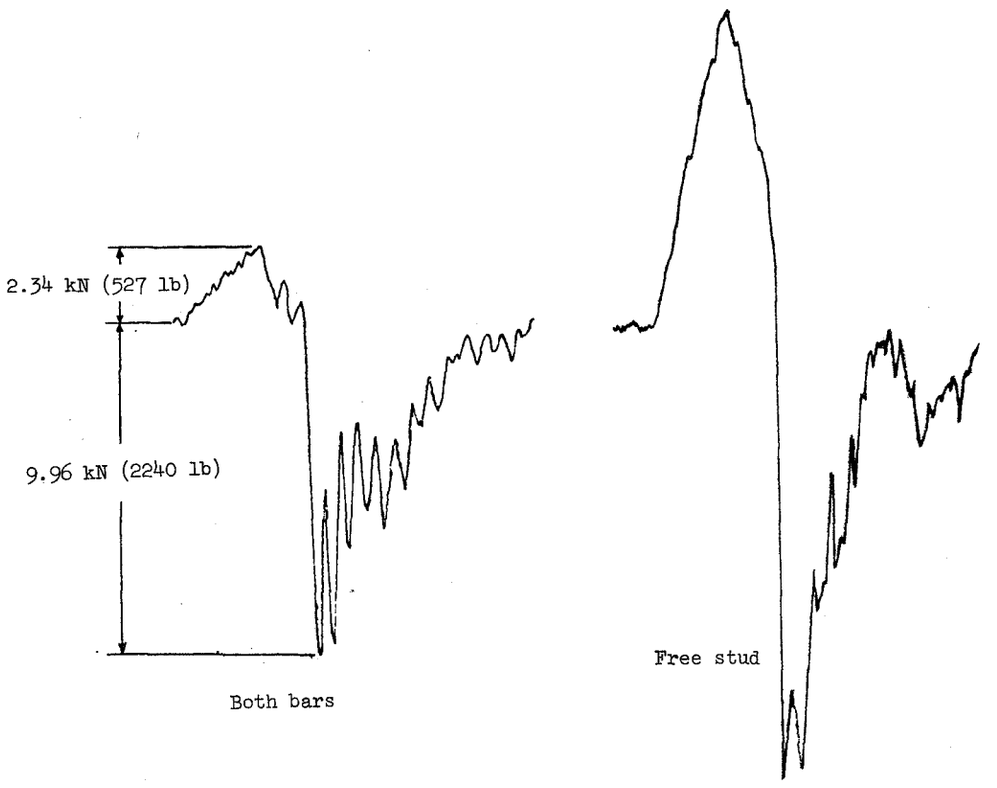

Figure 22.- Housing force performance comparison between using both bars and a free-stud (single bar) of Standard Design 1.

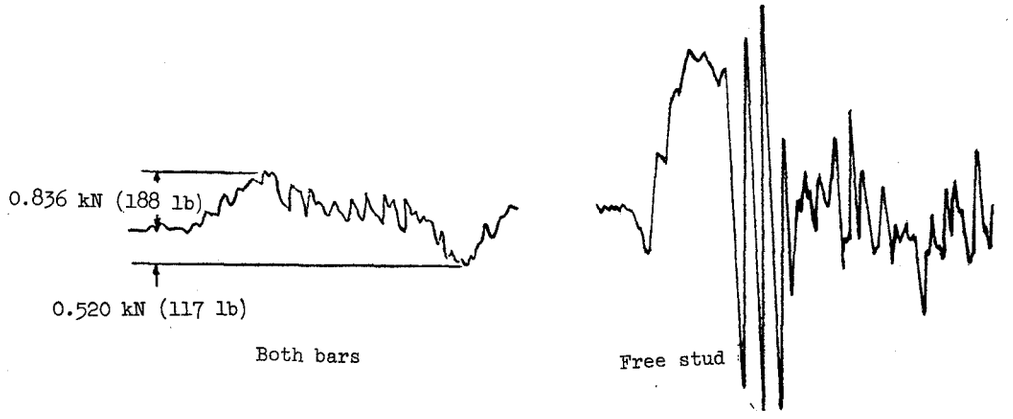

Figure 23.- Housing force performance comparison between using both bars and a free-stud (single bar) of Low-Shock Design 1.

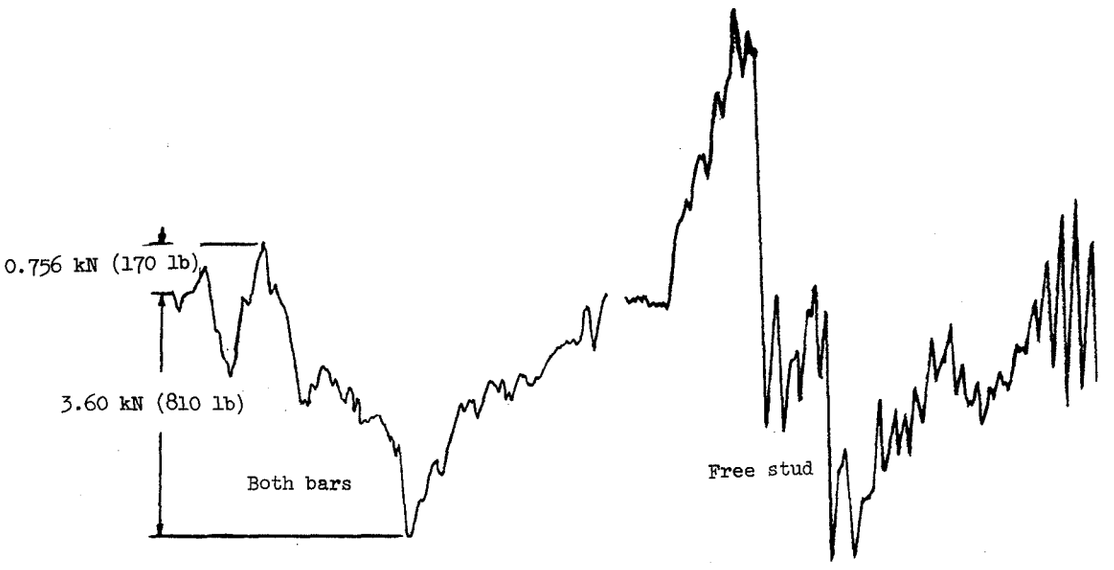

Figure 24.- Housing force performance comparison between two bars and a free-stud (single bar) of Low-Shock Design 2.

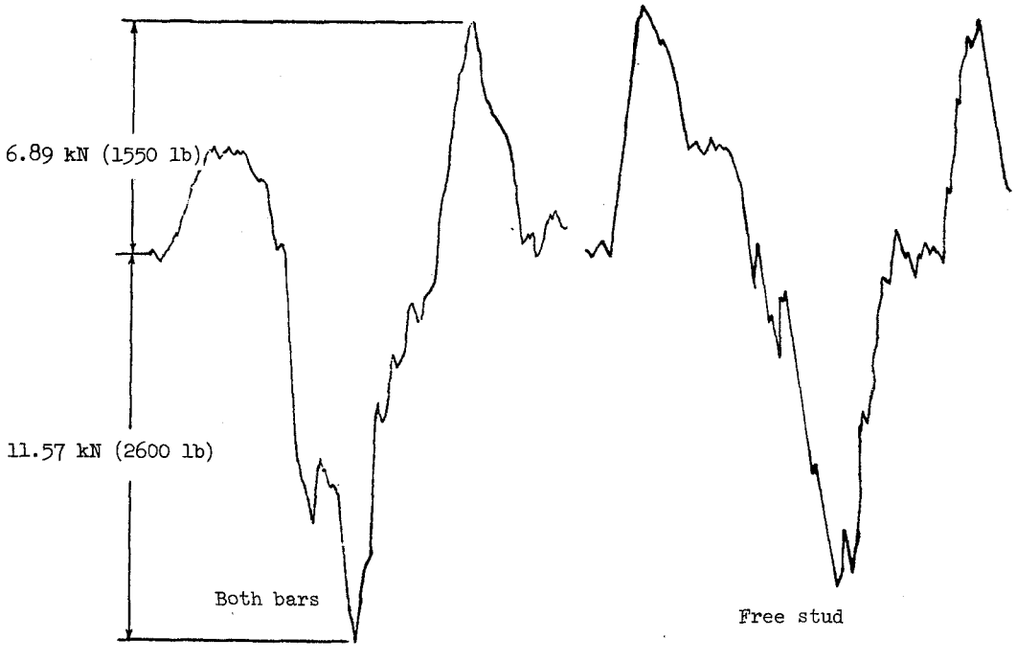

Figure 25.- Housing force performance comparison between two bars and a free-stud (single bar) of Low-Shock Design 3.

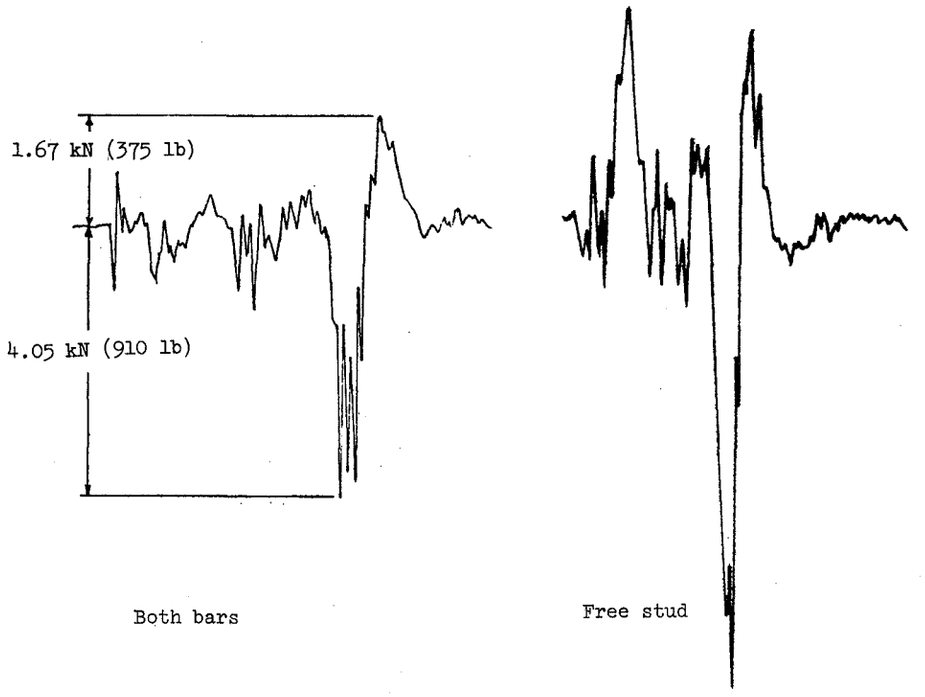

Figure 26.- Housing force performance comparison between two bars and a free-stud (single bar) of Low-Shock Design 4.

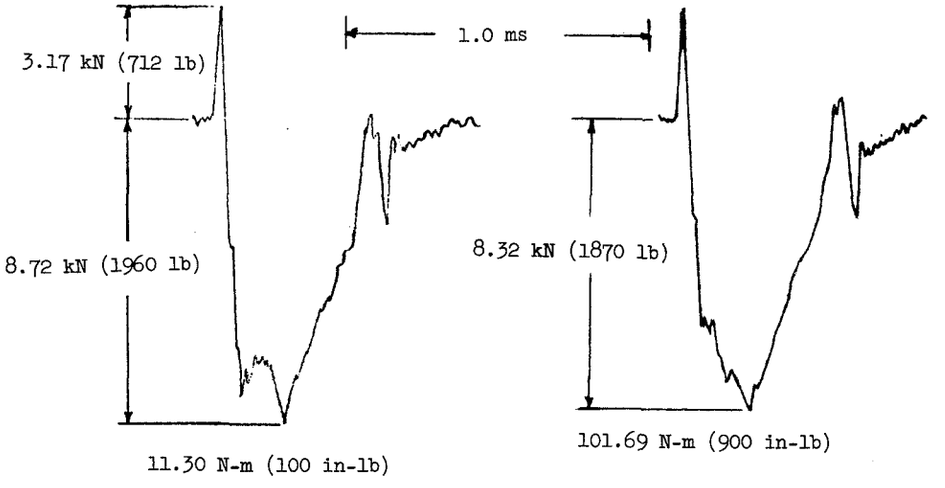

Figure 27.- Comparison of stud force performance for noncaptive nut at torque levels of 11.30 N-m (100 in-lb) and 101.69 N-m (900 in-lb).

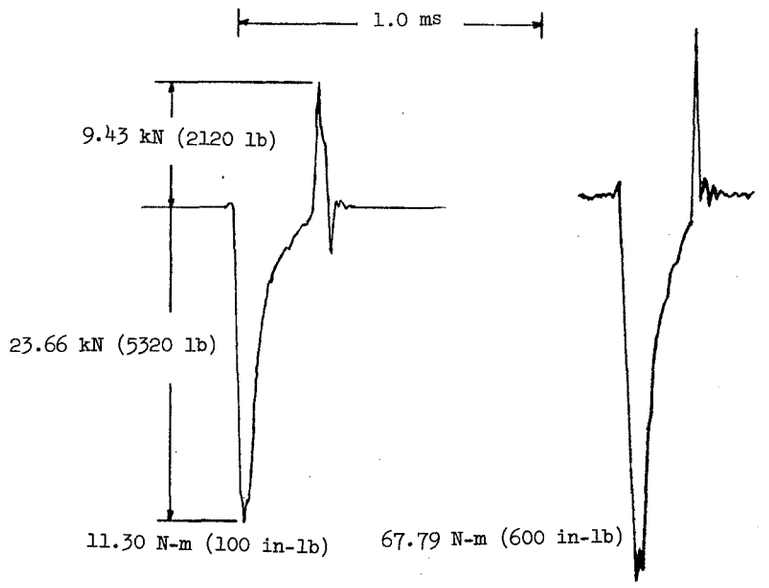

(a) Stud monitor.

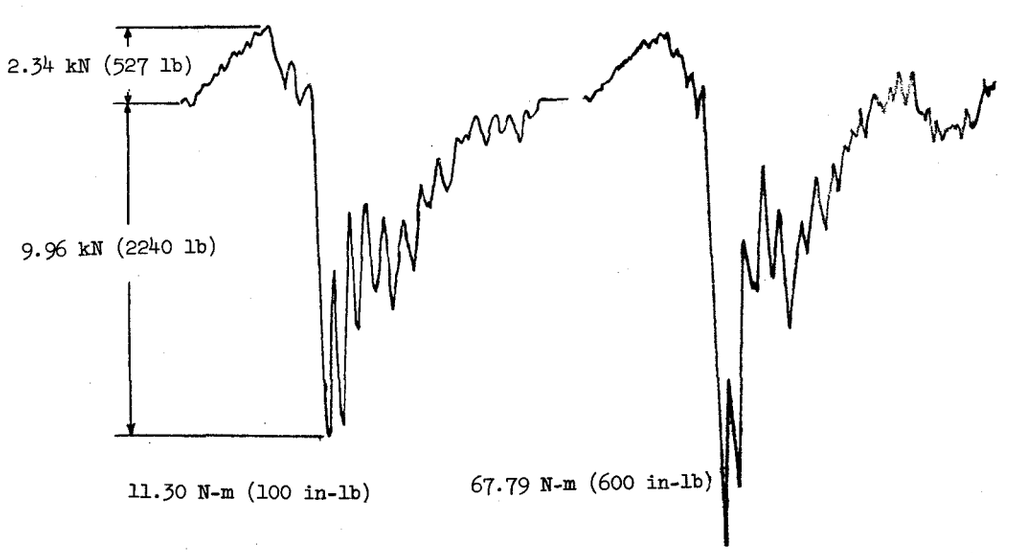

(b) Housing monitor.

Figure 28.- Comparison of force performances for Standard Design 1 at torque levels of 11.30 N-m (100 in-lb) and 67.79 N-m (600 in-lb).

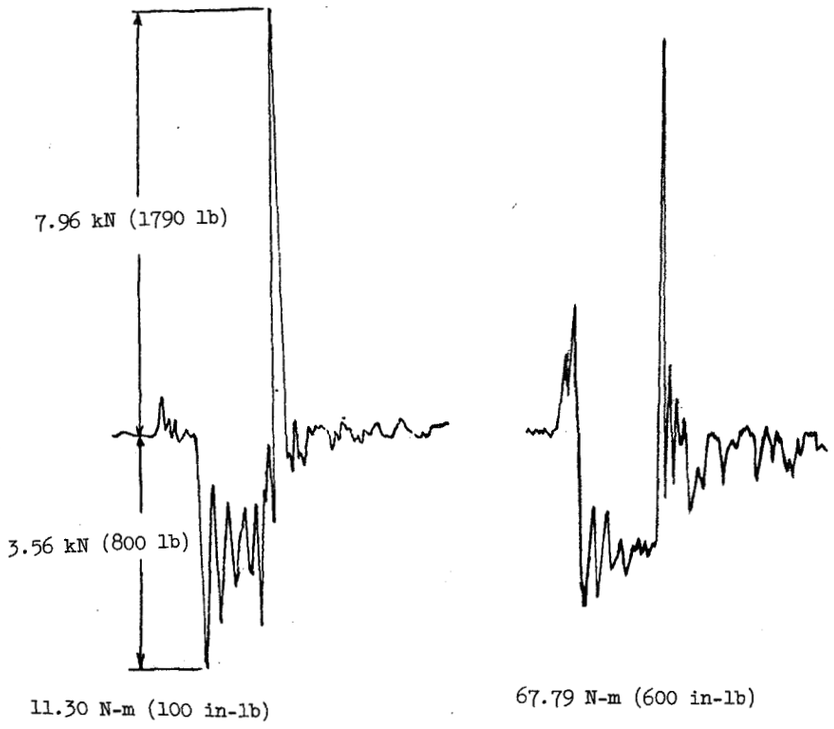

(a) Stud monitor.

(b) Housing monitor.

Figure 29.- Comparison of force performances for Low-Shock Design 1 at torque levels of 11.30 N-m (100 in-lb) and 67.79 N-m (600 in-lb).

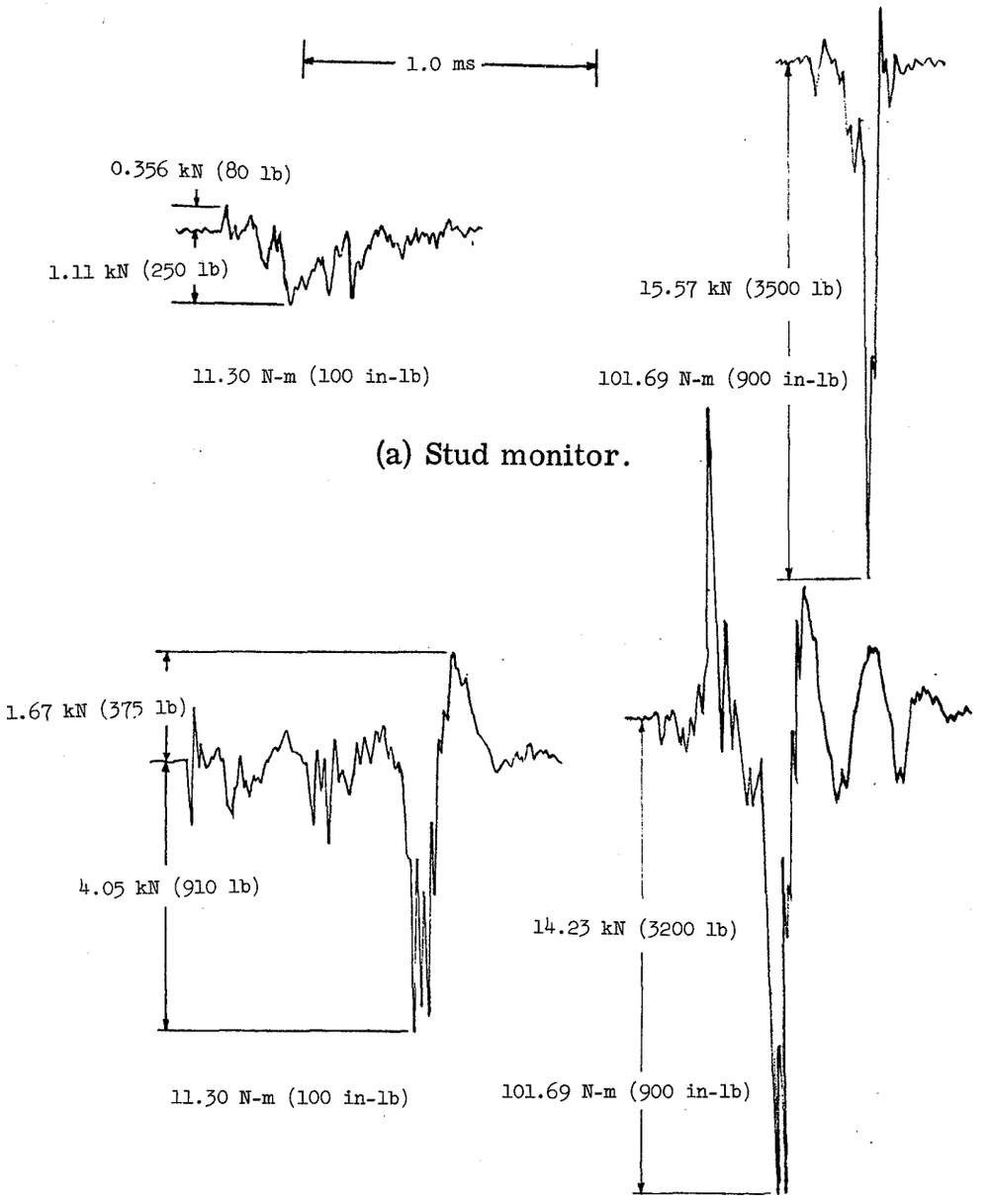

Figure 30.- Comparison of force performances for Low-Shock Design 4 at torque levels of 11.30 N-m (100 in-lb) and 101.69 N-m (900 in-lb).